Formation of three-dimensional cell aggregates expressing lens-specific proteins in various cultures of human iris-derived tissue cells and iPS cells

NORIKO HIRAMATSU[1,2*], NAOKI YAMAMOTO[1,3-5*], YU KATO[1,2], NORIAKI NAGAI[6], SUMITO ISOGAI[7] and KAZUYOSHI IMAIZUMI[7]

[1]Support Office for Bioresource Research, Research Promotion Headquarters; [2]Graduate School of Health Sciences; [3]International Center for Cell and Gene Therapy, Research Promotion and Support Headquarters, Fujita Health University, Toyoake, Aichi 470-1192; [4]Department of Ophthalmology; [5]Division of Vision Research for Environmental Health, Project Research Center, Medical Research Institute, Kanazawa Medical University, Kahoku, Ishikawa 920-0293; [6]Faculty of Pharmacy, Kindai University, Higashiosaka, Osaka 577-8502; [7]Department of Respiratory Medicine, School of Medicine, Fujita Health University, Toyoake, Aichi 470-1192, Japan

Received March 31, 2022; Accepted June 10, 2022

DOI: 10.3892/etm.2022.11476

Abstract. Induced pluripotent stem (iPS) cells are widely used as a research tool in regenerative medicine and embryology. In studies related to lens regeneration in the eye, iPS cells have been reported to differentiate into lens epithelial cells (LECs); however, to the best of our knowledge, no study to date has described their formation of three-dimensional cell aggregates. Notably, *in vivo* studies in newts have revealed that iris cells in the eye can dedifferentiate into LECs and regenerate a new lens. Thus, as basic research on lens regeneration, the present study investigated the differentiation of human iris tissue-derived cells and human iris tissue-derived iPS cells into LECs and their formation of three-dimensional cell aggregates using a combination of two-dimensional culture, static suspension culture and rotational suspension culture. The results revealed that three-dimensional cell aggregates were formed and differentiated into LECs expressing αA-crystallin, a specific marker protein for LECs, suggesting that the cell-cell interaction facilitated by cell aggregation may have a critical role in enabling highly efficient differentiation of LECs. However, the present study was unable to achieve transparency in the cell aggregates; therefore, we aim to continue to investigate the degradation of organelles and other materials necessary to make the interior of the formed cell aggregates transparent. Furthermore, we aim to expand on our current work to study the regeneration of the lens and ciliary body as a whole *in vitro*, with the aim of being able to restore focusing function after cataract surgery.

Correspondence to: Dr Naoki Yamamoto, Support Office for Bioresource Research, Research Promotion Headquarters, Fujita Health University, 1-98 Dengakugakubo, Toyoake, Aichi 470-1192, Japan
E-mail: naokiy@fujita-hu.ac.jp

*Contributed equally

Abbreviations: DMEM/F12, Dulbecco's modified Eagle's medium/Ham's F12; b-FGF, basic fibroblastic growth factor; ES cells, embryonic stem cells; H&E, hematoxylin and eosin; H-iris cells, human iris tissue-derived cells; H-iris iPS cells, human iris-derived iPS cells; IOLs, intraocular lenses; iPS cells, induced pluripotent stem cells; KSR, KnockOut™ serum replacement; LECs, lens epithelial cells; LFCs, lens fiber cells; PECs, pigmented epithelial cells; qPCR, quantitative PCR; SEAM, self-formed ectodermal autonomous multi-zone

Key words: iPS cells, LECs, H-iris cells, three-dimensional cell aggregate, p75NTR, αA-crystallin, type IV collagen, SEAM

Introduction

The development of the lens in the eye begins with the PAX6-expressing epidermal ectoderm making contact with the optic vesicle. Subsequently, SOX2 is expressed in the ectoderm region in contact with the optic vesicle, and the coordinated action of PAX6 as a partner factor for SOX2 causes cells in contact with the optic vesicle to thicken and form lens placodes, which are depressed inward by the formation of the optic cup (1). The lens placode is eventually separates from the epidermal ectoderm to form a spherical lens vesicle with an array of surrounding cells. Moreover, the cells that are positioned on the side of the lens follicle extend toward the interior of the lens placode and fill the interior (2,3).

The human lens is 9-10 mm in diameter and is surrounded by a lens capsule, which is rich in type IV collagen. On the corneal side, the lens epithelium is composed of a single layer of lens epithelial cells (LECs). Around the equatorial region of the lens, LECs separate from the capsule and begin to elongate toward the anterior and posterior poles of the lens, where the LECs differentiate into lens fiber cells (LFCs). Eventually, the organelles inside the LFCs disappear (4) and are replaced by

lens fibers filled with crystallin proteins. At the center of the lens lies the lens nucleus (fetal nucleus), which is formed during development and is surrounded by lens fibers (5). After birth, LECs continue to proliferate slowly, and the few remaining lens-tissue stem cells expressing p75NTR are suspected to be involved in proliferation (6). However, the proliferation of these cells slows with age (7).

The lens is composed of approximately 90% crystallin, a water-soluble protein. Crystallin in vertebrates is mainly classified into α-, β-, and γ-crystallin. α-crystallin has 2 subunits of αA- and αB-, β-crystallin has 7 subunits of βA1-βA4 and βB1-βB3, and γ-crystallin has 5 subunits of γA-γD and γS (8). In the lens, α-crystallin is a 40-mer, β-crystallin is a 2-6-mer, and γ-crystallin is a monomer, which play an important role in interacting with each other to maintain the transparency of the lens (9). α-crystallin is a major component of the lens, accounts for approximately 30% of the water-soluble protein in the lens, and functions as a molecular chaperone that suppresses aggregation of other crystallin species (10). In humans, αB-crystallin is expressed in tissues other than the eye, whereas αA-crystallin is expressed only in the lens (11). βB2-crystallin is the main component of β-crystallin. It has been reported that in βB2-crystallin obtained from the lens of senile cataract, the Asp residue at the C-terminal site undergoes significant site-specific isomerization, which occurs at the site of interaction with βB2-crystallin itself and other βB-crystallins, and it may contribute to the formation of senile cataract by affecting the crystallin subunit-subunit interaction and inducing abnormal crystallin aggregation (12).

After the lens of a newt is removed, the pigmented epithelial cells (PECs) located on the dorsal side of the iris first start to dedifferentiate, a process during which their pigment is degranulated, and then differentiate into LECs to regenerate a new lens (13,14). By contrast, regeneration of the lens in mammals does not occur once the lens capsule is removed (15). Intriguingly, if only the contents of the lens are removed and the lens capsule and LECs are preserved, the lens reproduces the same process as that occurring during embryonic development and forms a regenerated lens (16-18). However, the regenerated LECs exhibit aberrant, morphological changes, including irregular cell arrangement, mitochondrial degeneration, and vacuoles in the cytoplasm (19).

Induced pluripotent stem (iPS) cells, first described by Takahashi *et al* (20), are pluripotent cells that can differentiate into diverse cell types. Notably, iPS cells have also been reported to differentiate into LECs (21-24), but no study thus far has reported their formation of three-dimensional cell aggregates. Here, we investigated the formation of three-dimensional cellular aggregates expressing lens-specific proteins using human iris-derived tissue cells and iPS cells.

Materials and methods

Preparation of human iris tissue specimens. The tissues examined in the study were collected from patients with glaucoma during treatment with partial iris resection, and pieces of the collected human iris tissue were fixed in SUPER FIX™ rapid fixative solution (cat. no. KY-500; Kurabo Industries Ltd.) (6). Subsequently, paraffin sections were prepared from the fixed tissues by following standard procedures, and the sections were stained with hematoxylin and eosin (H&E). Iris samples were collected from patients who underwent partial iris resection as a treatment for glaucoma at the Department of Ophthalmology, Fujita Health University Hospital, between April 2015 and March 2017, and who consented to the study. The mean age of the patients was 58.9±5.4 years, 4 males and 7 females. Patients with ocular diseases other than glaucoma were excluded from the study. This study was performed with the approval (approval no. 05-065) of the Ethics Review Committee of Fujita Health University. The experiment was carried out with the approval (approval no. DP16055) of the Recombinant DNA Experiment Committee of Fujita Health University. All study participants provided written informed consent for their tissue to be used, and the study complied with the tenets of the Declaration of Helsinki for research involving human tissues.

Isolation and culture of cells from human iris tissue. Human iris tissue was processed as described (25,26). Briefly, iris tissue was treated with 0.2% collagenase (cat. no. C9722-50MG; Merck KGaA) and washed twice with phosphate-buffered saline (PBS; cat. no. D8662-500ML; Merck KGaA), and the isolated human iris tissue-derived cells (H-iris cells) were cultured in iris culture medium (iris medium): Advanced Dulbecco's modified Eagle's medium/Ham's F12 (Advanced DMEM/F12; cat. no. 12634010; Thermo Fisher Scientific Inc.) supplemented with 5% (w/v) mixed serum [heat-inactivated human serum (cat. no. H3667-20ML; Merck KGaA), KnockOut™ Serum Replacement (KSR; cat. no. 10828010; Thermo Fisher Scientific), and Artificial Serum, Xeno-free (cat. no. A2G10P2CC; Cell Science & Technology Institute, Inc.) in a 5:3:2 ratio], 10 ng/ml basic fibroblastic growth factor (b-FGF; cat. no. F0291; Merck KGaA), 10 ng/ml epidermal growth factor (cat. no. E9644; Merck KGaA), 1% (w/v) GlutaMAX™ (cat. no. 35050061; Thermo Fisher Scientific), 0.1% (w/v) CultureSure® Y-27632 solution (used only when starting the culture; cat. no. 039-24591; FUJIFILM Wako Pure Chemical Corporation), and 1% (w/v) penicillin/streptomycin (cat. no. P4458-100ML; Merck KGaA). The cells were plated in culture dishes coated with type I collagen (cat. no. TMTCC-050; Toyobo Co., Ltd.) and incubated at 37˚C in a 5% CO_2 humidified incubator, and the cultured cells were examined using an inverted fluorescence microscope equipped with a digital camera system (Power IX-71 and DP-71; Olympus Corporation).

Preparation of human iris-derived iPS cells. Human iris-derived iPS (H-iris iPS) cells were prepared through cell reprogramming using H-iris cells, as described previously (26). Briefly, H-iris cells were reprogrammed by employing a micro-electroporation method performed using an Epi5™ Episomal iPSC Reprogramming Kit (cat. no. A15960; Thermo Fisher Scientific) (27). After cloning, StemFit® (cat. no. RCAK02N; ReproCELL Inc.) mixed with 0.1% (w/v) CultureSure® Y-27632 solution (only at the beginning of culture) was used as the iPS cell-culture medium, and iMatrix-511 (Laminin-5; cat. no. 892011; Takara Bio Inc.) was used as the coating agent (STEP-0 culture condition; Fig. 1). During passaging, the H-iris iPS cells were detached using a mixture of Accutase (cat. no. AT104-100ML; M&S

TechnoSystems, Inc.) and TrypLE Select Enzyme (cat. no. 12563011; Thermo Fisher Scientific). The H-iris cells and H-iris iPS cells were confirmed to be negative for mycoplasma infection using a mycoplasma detection kit (EZ-PCR™ Mycoplasma Test Kit, cat. no. 20-700-20; Biological Industries USA Inc.) according to the manufacturer's instructions. The experiment was conducted with the approval (no. DP16055) of the Recombinant DNA Experiment Committee of Fujita Medical University.

Differentiation of H-iris cells and H-iris iPS cells into LECs. The composition of the used LEC medium (with the STEP-4 culture condition being the same; Fig. 1), which induces H-iris cells to differentiate into LECs, was as follows (28): 10% (w/v) fetal bovine serum (cat. no. 04-111-1A; Biological Industries Israel Beit-Haemek), 10 ng/ml b-FGF, 1% (w/v) minimum essential medium non-essential amino acids (cat. no. 11140050; Thermo Fisher Scientific), 0.5% (w/v) GlutaMAX™, DMEM high-glucose medium (cat. no. 11965092; Thermo Fisher Scientific), and 1% (w/v) penicillin/streptomycin solution.

The common differentiation culture conditions were based on reports describing the differentiation of human embryonic stem (ES) cells into lens progenitor cells and lentoid bodies (29); H-iris iPS cells were cultured in Lens differentiation base medium: Advanced DMEM/F12 supplemented with 0.05% (w/v) bovine serum albumin (cat. no. 012-23881; FUJIFILM Wako), 1% (w/v) non-essential amino acids (Thermo Fisher Scientific), 0.5% (w/v) GlutaMAX™, 0.5% (w/v) N-2 MAX Media Supplement (cat. no. 17502048; Thermo Fisher Scientific), 1% (w/v) B-27 supplement (cat. no. 17504044; Thermo Fisher Scientific), 100 ng/ml b-FGF, and 0.1% (w/v) CultureSure® Y-27632 solution, with 100 ng/ml Noggin (cat. no. 6057-NG; R&D Systems, Inc.) added for 6 days (STEP-1). On the 6th day, the medium was replaced with lens differentiation base medium containing 20 ng/ml bone morphogenetic protein-4/7 (cat. no. 3727-BP; R&D Systems) and 100 ng/ml b-FGF (STEP-2), and on the 18th day, this medium was replaced with lens differentiation base medium containing 20 ng/ml Wnt-3a (cat. no. 5036-WN; R&D Systems) and 100 ng/ml b-FGF (STEP-3).

Distinct culture environments were used in our experiments, Experiments 1-5 (Ex.1-Ex.5), as described below (summarized in Fig. 1): Ex.1: $1x10^5$ H-iris iPS cells were seeded into 3.5 cm adhesive cell-culture dishes coated with iMatrix-511 and cultured in iPS culture medium at 37˚C in a 5% CO_2 humidified incubator, and starting from the next day, the cells were maintained as adherent cultures sequentially under STEP-1, STEP-2, and STEP-3 culture conditions. Ex.2: $1x10^5$ H-iris iPS cells were seeded into 3.5 cm adhesive cell-culture dishes coated with iMatrix-511 and cultured in iPS culture medium at 37˚C in a 5% CO_2 humidified incubator, and from the next day, the cells were maintained as adherent cultures sequentially under STEP-1, STEP-2, and STEP-3 culture conditions. Under STEP-3 conditions applied for the last 10 days, the cells were detached using a mixture of Accutase and TrypLE Select Enzyme and cultured using the inclined rotational-suspension method in a centrifuge tube. Ex.3: $1x10^6$ H-iris iPS cells were cultured sequentially under the culture conditions of STEP-1 using the static-suspension method, STEP-2 using the inclined rotational-suspension method, and STEP-3 using the horizontal rotational-suspension method in a centrifuge tube. Ex.4: $1x10^6$ H-iris iPS cells were cultured in a centrifuge tube under STEP-1, STEP-2, and STEP-3 culture conditions sequentially using the static-suspension method and then using the inclined rotational-suspension method under STEP-4 conditions for 2 weeks. Ex.5 is described in the next subsection. The medium was changed every 2 days in Ex.1-Ex.5. For inclined rotation in the experiments, an NRC20D rotary mixer (Nissinrika Co., Ltd., Tokyo, Japan) was used at 3 rpm and a tilt angle of 45˚, and for horizontal rotation, an RT-50 rotator (TAITEC Corporation) was used at 35 rpm.

Differentiation of multiple ocular cells. As reported by Hayashi *et al* (30), H-iris iPS cells were cultured using the self-formed ectodermal autonomous multi-zone (SEAM) method for ocular cells (Ex.5). Briefly, H-iris iPS cells were seeded into iMatrix-511-coated cell-culture dishes at 350 cells/cm^2 using the StemFit® medium, and at 4 weeks after seeding, the culture medium (SEAM medium) was changed to the following differentiation medium: DMEM (cat. no. D5796-500ML; Merck KGaA) supplemented with 10% (w/v) KSR, 1% (w/v) sodium pyruvate (cat. no. 11360070; Thermo Fisher Scientific), 1% (w/v) non-essential amino acids, 1% (w/v) GlutaMAX™, 1% (w/v) monothioglycerol (cat. no. 195-15791; FUJIFILM Wako), and 1% (w/v) penicillin/streptomycin; the cells were cultured at 37˚C in a 5% CO_2 humidified incubator. The cells present in the area where LECs were observed using the SEAM method were harvested and cultured using the rotational-suspension method. After 4 weeks, the cell aggregates that formed between the 2nd and 3rd zones of the SEAM were picked using a pipette, cloned, and cultured in LEC medium, and then $1x10^6$ proliferated cells were cultured under the same conditions as in Ex.3 and differentiated into LECs.

Reverse transcription and quantitative PCR (qPCR). Total cellular RNA was extracted using a TaqMan® Gene Expression Cells-to-CT™ Kit (cat. no. A25603; Thermo Fisher Scientific), and RNA concentrations were measured using a spectrophotometer (NanoVue™; GE Healthcare) (31). Total RNA was reverse-transcribed using a GeneAmp® PCR System 9700 Thermal Cycler (Thermo Fisher Scientific) to synthesize cDNA, and, subsequently, qPCR was performed using an ABI PRISM® 7900 HT Sequence Detection System (Thermo Fisher Scientific) and the following primers and probes (TaqMan® Gene Expression assays; cat. no. 4331182; Thermo Fisher Scientific): *p75NTR* (assay ID. Hs00609976_m1), *SOX2* (assay ID. Hs00415716_m1), *PAX6* (assay ID. Hs01088114_m1), *type IV collagen* (assay ID. Hs00266237_m1), and the crystalline lens-marker gene *αA-crystallin* (assay ID. Hs00166138_m1); glyceraldehyde-3-phosphate dehydrogenase (*GAPDH*; assay ID. Hs99999905_m1) was used as an internal positive control. The thermocycling conditions were as follows: reverse transcription: 60 min at 37˚C and 5 min at 95˚C. qPCR: 2 min at 50˚C, 10 min at 95˚C, 15 sec at 95˚C and 1 min at 60˚C, for 50 cycles. Relative expression was analyzed by the delta-delta Ct method using Ct values obtained from qPCR amplification.

Sectioned specimens of cell aggregates. Cell aggregates were collected from suspension cultures and treated using the cell-block method (32) to prepare paraffin-section specimens using a fixative solution as described previously.

Immunofluorescence staining. Immunofluorescence staining was performed as previously described (26,33). Briefly, fixed cells were permeabilized with 0.5% Triton X-100 (cat. no. 04605-250; FUJIFILM Wako), blocked with a serum-free ready-to-use blocking reagent (cat. no. X090930-2; Agilent Technologies, Inc.) for 5 min at room temperature, and stained with one of the following primary antibodies (incubated for 1 h at 37˚C): anti-human αA-crystallin rabbit polyclonal antibody (1:100; cat. no. ab5595; Abcam plc.), anti-human PAX6 mouse monoclonal antibody (1:100; cat. no. 14-9914-80; Thermo Fisher Scientific), anti-human SOX2 rat monoclonal antibody (1:100; cat. no. 14-9811-82; Thermo Fisher Scientific), anti-human type IV collagen rabbit polyclonal antibody (1:200; cat. no. LB-0445; Life Science Laboratories, Inc.), anti-p75NTR rabbit polyclonal antibody (1:200; cat. no. ANT-007; Alomone Labs), and anti-human βB2-crystallin rabbit polyclonal antibody (1:100; cat. no. ab252971; Abcam). Next, the cells were incubated with an appropriate secondary antibody, Alexa Fluor 594-labeled anti-mouse IgG donkey antibody (1:500; cat. no. A-21203; Thermo Fisher Scientific), Alexa Fluor 594-labeled anti-rabbit IgG goat antibody (1:500; cat. no. A-11037; Thermo Fisher Scientific), or Alexa Fluor 594-labeled anti-rat IgG goat antibody (1:500; cat. no. A-11007; Thermo Fisher Scientific), for 1 h at 37˚C. DAPI (VECTASHIELD Mounting Medium with DAPI; cat. no. H-1200; Vector Laboratories) was used for nuclear staining. The immunostaining was evaluated using a fluorescence microscope (Power BX-51; Olympus).

Statistical analysis. Each experiment was performed in triplicate and repeated at least thrice. Data are presented as means ± standard deviation (SD) and were analyzed using repeated measures analysis of variance with Tukey's post hoc test. Statistical Package for Social Science (SPSS) Statistics 24 (IBM Corporation) was used for statistical analyses.

Results

Primary culture and differentiation of H-iris cells. Human iris tissue was enzymatically treated and decomposed into small pieces (Fig. 2A). Cells proliferated from the tissue pieces that adhered to dishes (Fig. 2B), and while some of these cells contained a pigment in the cytoplasm, the pigment was degranulated in several cells (Fig. 2C). On Day 7 of culture, the cells became confluent and the cultures included very few pigmented cells (Fig. 2D). After culturing in STEP-4 medium for 3 weeks, the cultures contained small cell masses (lentoid body-like masses) in which the cells were partially aggregated (Fig. 2E). When the small cell aggregates were collected using a pipette and immunostained with an αA-crystallin antibody, numerous brightly stained cells were observed (Fig. 2F-H).

Differentiation using the Ex.1 method. When iPS cells cultured in iPS medium (Fig. 3A) were cultured in STEP-1 medium for 6 days, cells featuring short protrusions were observed (Fig. 3B). After 12 days in STEP-2 medium, the cells were fully confluent and partially multilayered (Fig. 3C), and after 17 days in STEP-3 medium, the cells were further multilayered (Fig. 3D). On the last day of culture of each step from STEP-0 to STEP-3, the cells were collected and total RNA was extracted and reverse-transcribed to produce cDNA for PCR analyses; our results showed that *p75NTR* mRNA expression levels were significantly higher at STEP-1, -2, and -3 than at STEP-0 (Fig. 3E). Moreover, at STEP-3, the cultures included a few αA-crystallin-positive cell populations, and the αA-crystallin-positive cells were negative for SOX2 (Fig. 3F-I).

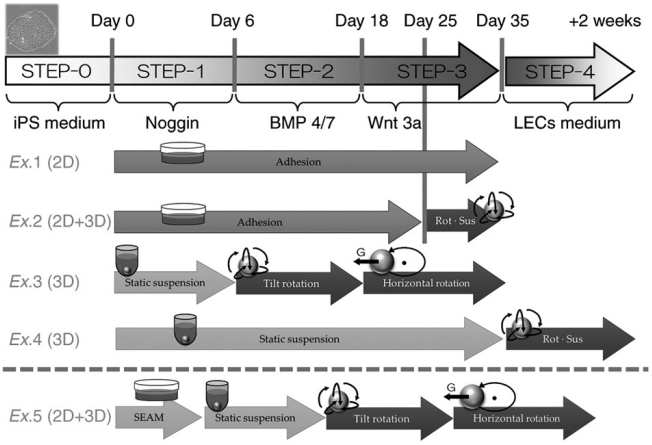

Figure 1. Schematic of cell-culture conditions in Ex. 1-5. iPS, induced pluripotent stem; LECs, lens epithelial cells; Rot·Sus, rotational suspension; Ex, experiment; 2D, 2-dimensions; 3D, 3-dimensions; SEAM, self-formed ectodermal autonomous multi-zone.

The expression of PAX6, SOX2, and αA-crystallin proteins at each step was confirmed through immunostaining performed under identical conditions. The expression of αA-crystallin was strongest at STEP-3, but the expression was not uniform, with certain cells expressing the protein more strongly than others, and the expression tended to be stronger in aggregated cells than in non-aggregated cells (Fig. 4). Fig. 4 examines the changes in protein expression of PAX6, SOX2, and αA-crystallin during lens development *in vivo* at different culture steps. Since iPS cells were used in this study, SOX2, one of the markers of iPS cells, is strongly expressed in STEP-0. However, by starting the induction of differentiation to lens, the expression of SOX2 decreased once in STEP-1, but as the differentiation STEP to lens progressed, the expression of SOX2 became strong again. On the other hand, PAX6 was slightly expressed in STEP-1. In addition, αA-crystallin, a marker of lens protein, was hardly detected until STEP-2, but was strongly detected in STEP-3, indicating that the cells differentiated into lens epithelial cells.

Differentiation using the Ex.2 method. The Ex.2 method was the same as the Ex.1 method until the end of STEP-2, but in STEP-3, starting from 7 days after initiation of the culture, the cells were cultured on a rotary culture device (Fig. 5A). After 10 days of this rotational suspension culture, opaque cell aggregates were formed (Fig. 5B). Sections of the cell aggregates were prepared using the cell-block method, and

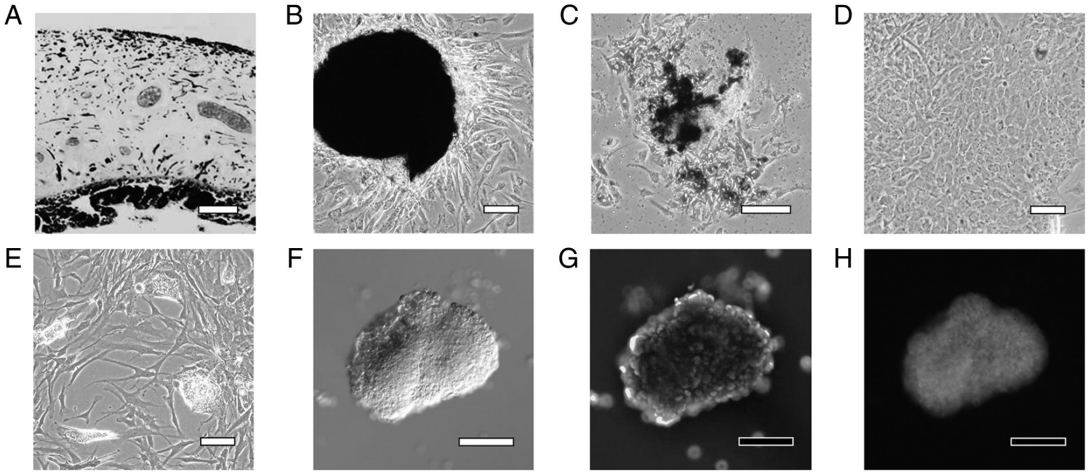

Figure 2. Formation of lentoid body-like cell aggregates from human iris tissue-derived cells. (A) H&E-stained specimen of human iris tissue. The pigment epithelial cell layer on the lens side is thick, and a thin pigment epithelial cell layer is also present on the corneal side. The iris parenchyma is composed of blood vessels, smooth muscle, and fibroblasts. (B) Fibroblasts and pigment epithelial cells have extended out from the enzyme-treated tissue. (C) Pigment epithelial cells proliferate while degranulating. (D) When only degranulated epithelial cells were passaged, the cells eventually became confluent with a cobblestone-like appearance. (E) Cells aggregated to form a lentoid body-like cell mass. (F) Morphology of the picked-up cell mass by micropipette. (G) DAPI staining of the cell mass in (F). (H) αA-crystallin staining of the cell mass in (G); the cytoplasm is stained here. Scale bar, 100 μm. H&E, hematoxylin and eosin.

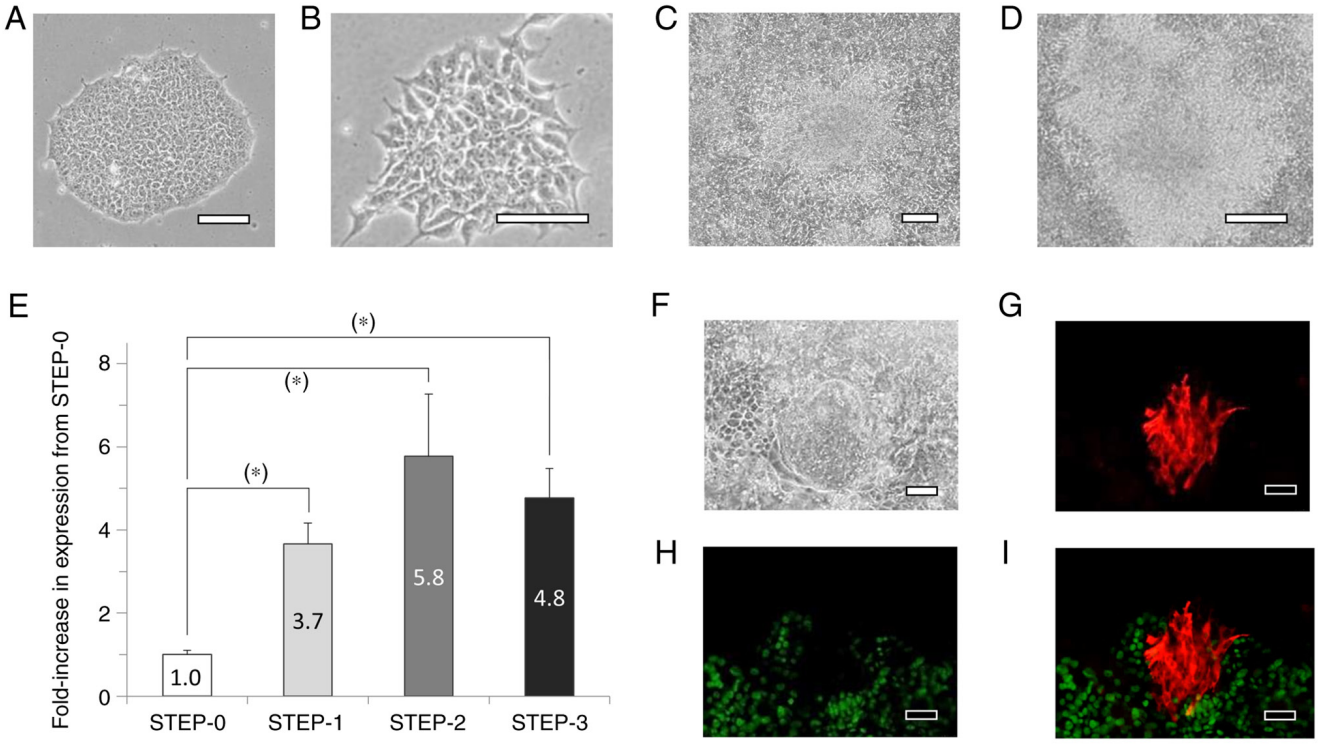

Figure 3. Induction of differentiation using the Ex.1 method. (A) Colony of human iris-derived iPS cells. (B-D) Cell colony in differentiation culture: (B) 6th day in STEP-1 medium, (C) 18th day in STEP-2 medium, and (D) 25th day in STEP-3 medium. Scale bar in (A-D), 100 μm. (E) Fold-increase in *p75NTR* mRNA expression level at different steps relative to STEP-0: *P<0.05. (F) Cell morphology on 35th day of differentiation in STEP-3 medium. (G) Immunostaining for αA-crystallin in the same area as indicated in (F). (H) Immunostaining for SOX2 in the same area as in (G). (I) Merged image of αA-crystallin and SOX2 immunostaining. Scale bar in (F-I), 100 μm. Ex, experiment; iPS cells, induced pluripotent stem cells.

H&E staining revealed that the aggregates were surrounded by one or two layers of cells, with the aggregate interior being filled with cells distinct from the cells around the aggregates (Fig. 5C). Moreover, the cells forming the aggregates showed cytoplasmic staining for αA-crystallin (Fig. 5D and E). An illustration of the developmental process of the lens is presented in Fig. 5F. Initially, a lens follicle featuring a hollow center is formed, and then the interior of the follicle is filled with cells extending from one direction on the optic cup side.

Differentiation by the Ex.3 method. In the Ex.3 method, cell aggregates were formed starting from the STEP-1 stage, with differentiation occurring in the cell aggregates, and several days after the start of culture in STEP-3, numerous

sac-like structures were observed around the cell aggregates (Fig. 6A and B). The sac-like structures were translucent (Fig. 6C), and H&E staining of cell-block sections revealed that these structures were formed by two layers of cell membranes, with the inner layer being hollow (Fig. 6D). The two cell layers showed identical staining for αA-crystallin (Fig. 6E), although the outer cells showed stronger type IV collagen staining than did the inner cells (Fig. 6F). Conversely, in H&E staining of the cell aggregates, we observed that these structures were formed by two layers of cells, and cells whose nuclei were larger and cytoplasm was darkly stained with eosin were observed compared to the sac-like structures (Fig. 6G). The cells whose cytoplasm was darkly stained with eosin were also strongly positive for αA-crystallin (Fig. 6H) and type IV collagen (Fig. 6I) in both the inner and outer layers of the two-layer structure.

Differentiation using the Ex.4 method. In the Ex.4 method, cells were cultured using the static-suspension method to allow the formation of cell-cell junctions for differentiation. Subsequently, a step involving rotational suspension culture, STEP-4, was included for an additional 2 weeks. Expression analysis of five genes revealed that the expression levels in STEP-3 and STEP-4 were significantly higher than the changes between STEP-0 and STEP-1 and STEP-2 (Fig. 7A-E). The expression levels of *p75NTR* and type IV collagen were significantly higher in STEP-3 than in STEP-0, with the expression levels of the two genes decreasing in STEP-1 as compared to the level in STEP-0 but increasing thereafter. The expression levels of *SOX2* and *PAX6* increased during ocular differentiation, and in the Ex.4 method, the expression levels of these genes were significantly increased in STEP-3 and STEP-4.

Visual examination of cell aggregates obtained at the end of culture (Fig. 8A) revealed that the aggregates were milky-white and opaque, although the opacity was lighter in certain areas than in others. The results of H&E staining of sectioned specimens further showed that vacuoles formed inside the cell aggregates (Fig. 8B). Moreover, the surface of the cell aggregates was stratified, as illustrated in Fig. 8C showing an enlarged view of Area 1 from Fig. 8B, and these cells were positive for SOX2 (Fig. 8D), p75NTR (Fig. 8E), αA-crystallin (Fig. 8F), and type IV collagen (Fig. 8G). Conversely, in the region that is marked as Area 2 in Fig. 8B and enlarged in Fig. 8H, the cells on the surface of the aggregates transitioned from multilayers to monolayers, and the monolayers were negative for SOX2 (Fig. 8I); furthermore, in this region, p75NTR expression was decreased (Fig. 8J), and αA-crystallin staining was not detected (Fig. 8F), but positive staining for type IV collagen was observed (Fig. 8G).

Differentiation using the Ex.5 (SEAM) method. H-iris iPS cells (Fig. 9A) were cultured continuously for 4 weeks in a differentiation medium of the same composition. At the end of culture, small cell aggregates were observed at the boundary between the 2nd and 3rd zones (Fig. 9B), and these aggregates were positive for αA-crystallin (Fig. 9C). The cell aggregates were carefully harvested using a pipette and cultured using the static- and rotational-suspension methods. H&E staining of sections of the cell aggregates revealed that the cells were arranged in concentric circles, and in the cells in the interior of the aggregates, the cytoplasm was uniformly stained with eosin (Fig. 9D). αA-crystallin staining was detected in the cells surrounding the aggregates and in the inner cells whose cytoplasm was stained with eosin (Fig. 9E), and βB2-crystallin staining was slightly stronger in the inner cells than in the cells around the aggregates (Fig. 9F). Moreover, the cells around and inside the cell aggregates were positive for type IV collagen, and the inner cells whose cytoplasm was uniformly stained with eosin also particularly stained strongly for type IV collagen (Fig. 9G).

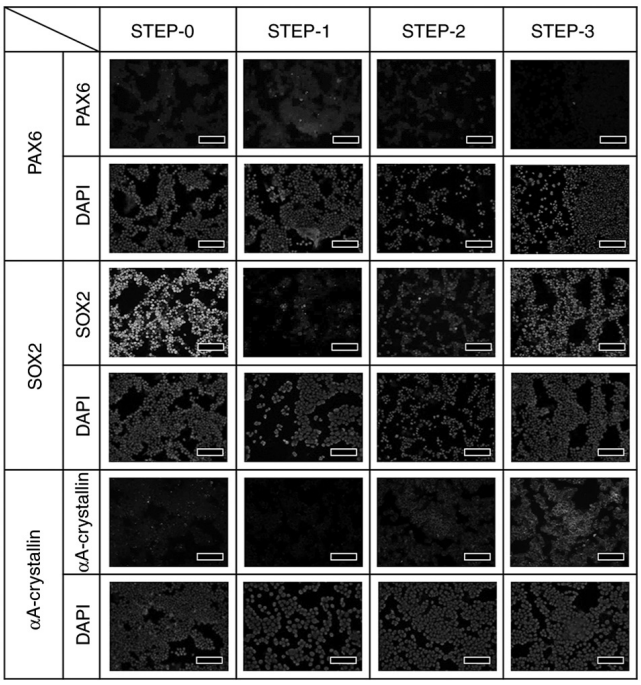

Figure 4. Immunostained specimens from each of the four steps in the Ex.1 method. The images show DAPI staining in the same area as that stained for PAX6, SOX2, and αA-crystallin in STEP-0, -1, -2, and -3. Scale bar, 100 μm. Ex, experiment.

Discussion

In this study, we cultured human iris-derived tissue cells and iPS cells using various culture methods and generated three-dimensional cell aggregates expressing αA-crystallin, a lens-specific protein.

The history of research on lens regeneration began with lens regeneration in newts, which was discovered in the 1890s (34,35). In newts, when the lens is removed, the pigment in the iris degranulates and then the iris tissue regenerates the lens. Lens regeneration in newts is unique, with the lens being unfailingly regenerated from the dorsal iris. Studies conducted using transgenic newts have shown that b-FGF and Wnt play a major role in the regeneration of the lens, refuting the notion that tissue stem cells exist only in the dorsal iris (36), and lens regeneration has also been shown to occur several times during the lifetime of a newt (13,37). However, no study to date has reported lens regeneration from the iris in mammals. We have been conducting research in the field of regenerative medicine with a focus on iris tissue (38-41). Here, we found that lentoid body-like cell aggregates expressing a very small but lens-specific protein

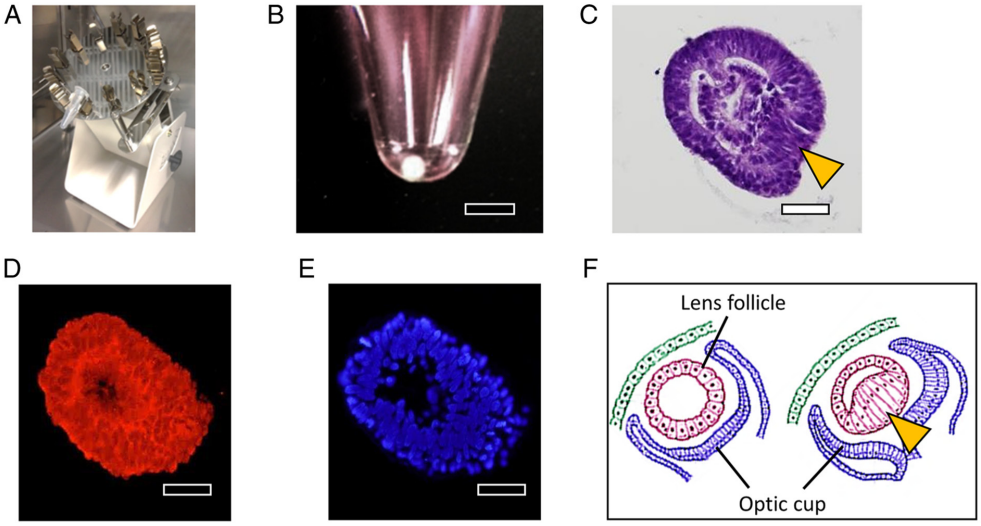

Figure 5. Induction of differentiation using the Ex.2 method. (A) System used for rotational suspension culture. (B) Opaque cell aggregates formed during culture. Scale bar, 2 mm. (C) H&E-stained specimen of cell aggregate, showing inward extension of pericytes (arrowhead). (D) Cell aggregate immunostained for αA-crystallin; the cytoplasm is stained. (E) DAPI staining of specimen shown in (D). Scale bar in (C-E), 100 μm. (F) Illustration of the lens during development. Ex, experiment; H&E, hematoxylin and eosin.

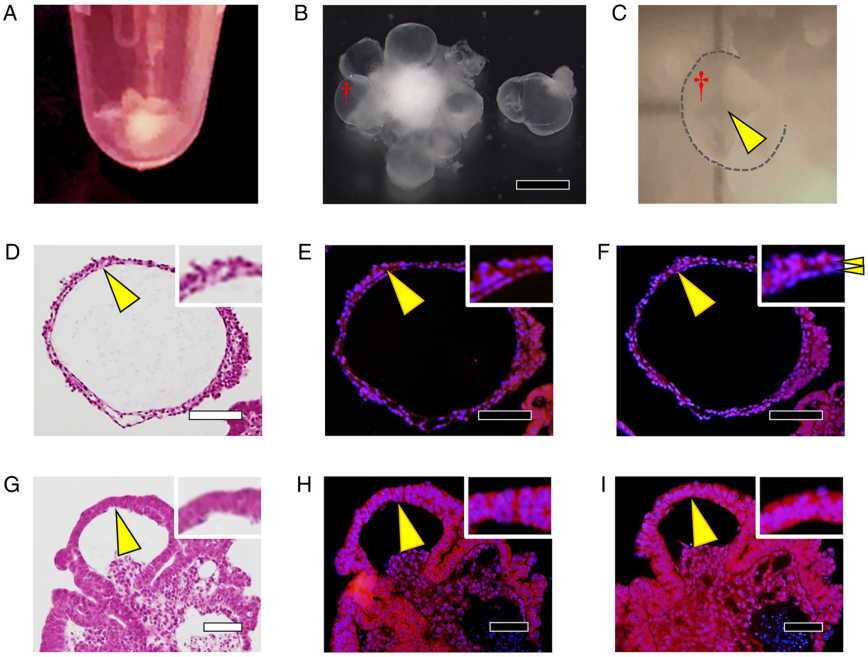

Figure 6. Induction of differentiation using the Ex.3 method. (A) Cell aggregates formed by using rotational suspension culture. (B) A sac-like structure (†) is observed here around the cell aggregate. Scale bar, 2 mm. (C) The sac-like structure (†) is translucent, and thus the black crosshairs are visible through it (arrowhead). (D) H&E-stained specimen of the sac-like structure. (E) Immunostaining for αA-crystallin in the sac-like structure. (F) Immunostaining for type IV collagen in the sac-like structure. (G) H&E-stained specimen of cell aggregate. (H) Immunostaining for αA-crystallin in cell aggregate. (I) Immunostaining for type IV collagen in cell aggregate. (D-I) inset: magnified view of area indicated by the arrowhead. Scale bar in (D-I), 100 μm. Ex, experiment; H&E, hematoxylin and eosin.

were formed in cultures of cells derived from human iris tissue. We previously reported that cultured H-iris cells included cells positive for tissue stem cell markers (CD271 and p75NTR) (26), and p75NTR is also a tissue stem cell marker in the lens (42). Our method of culturing iris tissue can also be used to culture certain cells that are positive for tissue stem cell markers, and this is the first report of PECs in human iris tissue degranulating and differentiating into small cell aggregates (lentoid body-like cell masses) expressing αA-crystallin, a marker for LECs.

First, we cultured H-iris iPS cells to induce their differentiation into lens epithelial progenitor cells based on a report that ES cells can differentiate into these progenitor cells (29). As compared to the iPS cells at STEP-0, the progressively differentiating cells showed increasing mRNA expression of *p75NTR*, a marker of lens epithelial stem cells. Moreover, PAX6 protein expression increased during STEP-1, the stage at which *p75NTR* mRNA expression started to increase, whereas SOX2 protein expression decreased once during

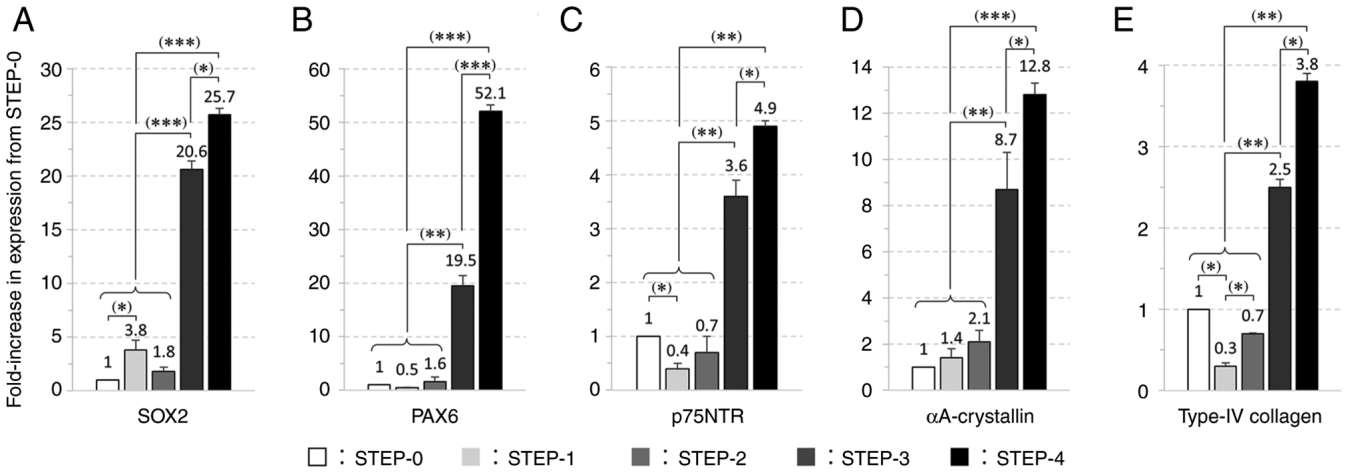

Figure 7. Changes in gene expression levels at each step of differentiation induction using Ex.4 the method. (A) *SOX2*, (B) *PAX6*, (C) *p75NTR*, (D) *αA-crystallin*, (E) *type-IV collagen*; fold-changes are relative to gene expression level in STEP-0: *P<0.05, **P<0.01, ***P<0.005. Ex, experiment.

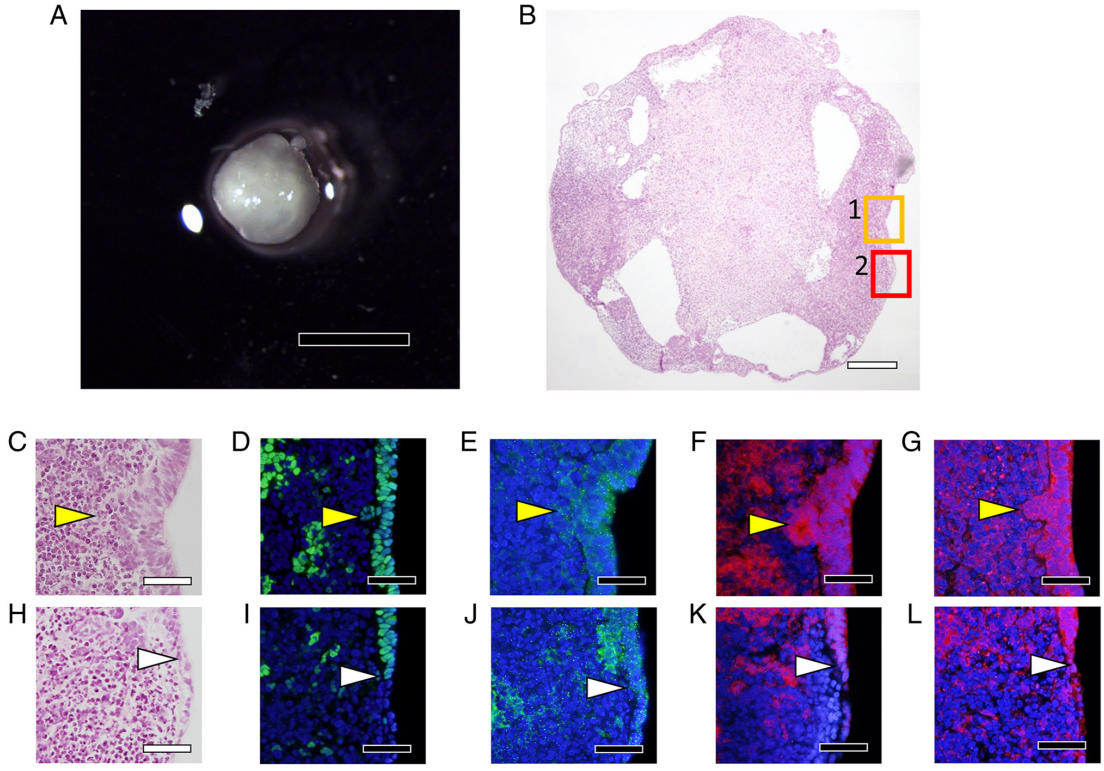

Figure 8. Induction of differentiation using the Ex.4 method. (A) Gross observation of cell aggregate. Reduced opacity is observed in certain areas. Scale bar, 2 mm. (B) H&E-stained specimen of cell aggregate. Scale bar, 200 μm. (C) Enlarged view of H&E staining in Area 1 of the specimen in (B). Cells displaying epithelial-like morphology have infiltrated inside the cell aggregate (yellow arrowhead). (D-G and I-L) Immunostaining of cell aggregates for (D and I) SOX2, (E and J) p75NTR, (F and K) αA-crystallin, and (G and L) type IV collagen. Blue in immunostaining images: DAPI staining of nuclei. (H) Enlarged view of H&E staining of Area 2 in the specimen in (B), where the cells on the surface of the aggregate have transitioned from a multilayer to a monolayer (white arrowhead). Scale bar in (C-L), 50 μm. Ex, experiment; H&E, hematoxylin and eosin.

STEP-1 and increased again during STEP-3. The association between *PAX6* and *SOX2* is critical because the two have been reported to act in conjunction to activate the expression of *δ-crystallin* and induce the development of lens placodes (1). Cells expressing αA-crystallin protein were observed during STEP-3, where crystallin-positive cells were aggregated and not all cells expressed αA-crystallin. Cell-cell interactions could play a crucial role in lens differentiation by inducing the formation of cell aggregates.

The maturation of cartilage cells has been reported to be promoted by the application of a mechanical stimulation or load to cells, and cellular aggregates generated using rotational culture have been proposed to represent an essential component for creating artificial cartilage through tissue engineering (43-47). Here, from the middle of STEP-3, when rotational suspension culture was performed as a mechanical stimulus (Ex.2), the cell aggregates formed were surrounded by one or two layers of cells, and cells elongating inward from

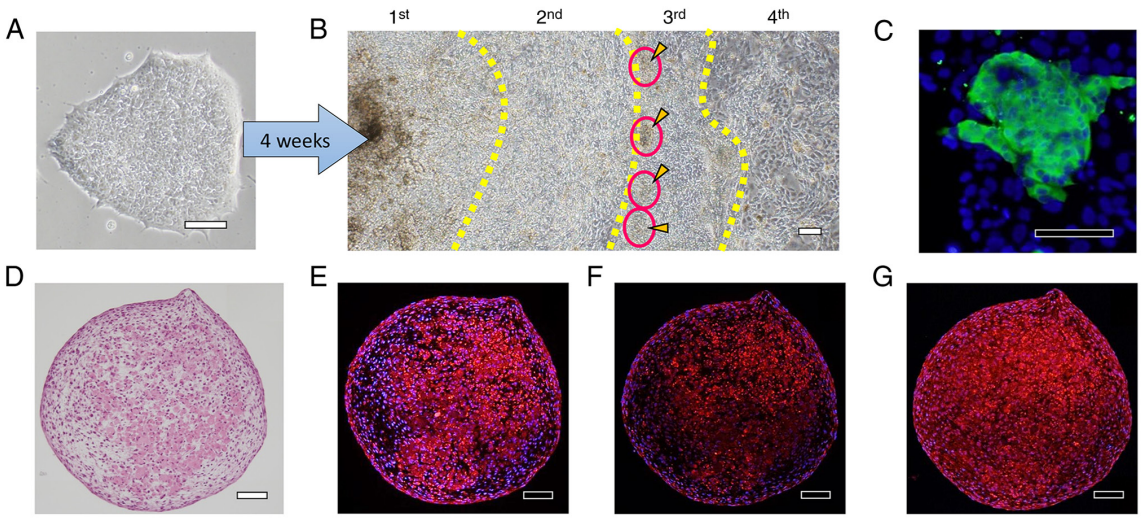

Figure 9. Induction of differentiation using the Ex.5 method. (A) iPS cell colony immediately before medium replacement with SEAM medium. (B) Colony after culture for 4 weeks in SEAM medium. Cell morphology can be distinguished into four layers from the center. At the boundary between the 2nd and 3rd zones, small cell aggregates were observed (arrowhead). (C) αA-crystallin immunostaining of a small cell mass indicated by arrowhead in (B). (D) H&E staining of cell aggregate after static and rotational suspension culture. (E-G) Immunostaining of cell aggregate for (E) αA-crystallin, (F) βB2-crystallin, and (G) type IV collagen. Blue: DAPI staining of nuclei. Scale bar, 100 μm. Ex, experiment; iPS cells, induced pluripotent stem cells; SEAM, self-formed ectodermal autonomous multi-zone; H&E, hematoxylin and eosin.

certain directions were observed to fill the interior of the aggregates. Our finding is similar to the observed proliferation and migration of cells during lens formation during development, and these cells expressed αA-crystallin. However, the cell aggregates grew to <1 mm as the largest size.

Considering the aforementioned results, we next cultured cells by employing the cell aggregates from STEP-1 and subjecting them to tilt rotation and horizontal rotation (Ex.3). Translucent sac-like structures formed by two layers of cell membranes were observed. In the sac-like structures, type IV collagen was strongly expressed outside the bilayer, mimicking the type IV collagen-rich lens capsule present on the outer surface of the lens (48-50). However, because the process of development and growth of the lens capsule remains unclear, embryological and cell-based studies on the lens capsule are required.

As the next method, STEP-4 using LEC medium was performed (Ex.4). All measured gene expression increased during STEP-3 and further increased in STEP-4. The cell aggregates grew to ~2 mm in size, with the surrounding cells, including LECs, arranged in the same manner as in the lens in certain areas, and a few vacuolated areas were present in the interior.

Lastly, in Ex.5, the areas where LECs formed in differentiated SEAM were collected and cultured. The SEAM method is a two-dimensional adhesion-culture method, and the concentric SEAMs formed by cells differentiating on their own through cell-cell interaction without changing the medium conditions mimic the development of the whole eye: the location of cells in different zones shows lineages spanning the superficial ectoderm, lens, neural retina, and retinal pigment epithelium of the eye. When cells in the areas where superficial ectoderm differentiate under the SEAM method are collected and further differentiated using the air-lift method, a three-dimensional cell sheet expressing proteins characteristic of the corneal and conjunctival epithelium is formed (23,30,51). Therefore, in the case of cells differentiated according to the SEAM regions, differentiation is induced in a manner that is highly distinct from the differentiation triggered previously in iPS cells using other methods. A relatively uniform interior was detected in the cell aggregates generated by collecting αA-crystallin-positive cells formed using the SEAM method and then culturing them using static- and rotational-suspension methods, and βB2-crystallin and type IV collagen positivity was also detected. However, no lens capsule was observed in these cell aggregates. It could be challenging to completely control the directionality of cell arrangement in cell aggregates without a lens capsule being present as a basement membrane.

The lens nucleus is located at the center of the lens, where organelles are lost during development. A recent study on organelle degradation inside the lens reported that organelle degradation by phospholipases of the PLAAT family leads to the achievement of optimal transparency and refractive function of the lens (4). Organelles affect light scattering, and in a flow cytometer, a widely used research instrument, the measurement is based on the principle that laterally scattered light is affected by the size of the cell nucleus and the presence of cell membranes and organelles (52,53). We speculate that one of the reasons why the cell aggregates produced in this study were not transparent is that intracellular organelles remained and affected light scattering.

In the case of cataracts, a disease that causes opacity of the lens, several artificial lenses (intraocular lenses; IOLs) have been developed through micro-incisions and are being used for clinical treatment. Regeneration of the lens *in vitro* is highly intriguing as a basic research subject, but for clinical application, the regeneration achieved must offer advantages over current IOL-based treatments. Multifocal IOLs that can focus at distinct distances are also being developed for clinical use. In cataract surgery, the lens capsule is preserved and only the opaque lens is emulsified using ultrasound and then suctioned out. However, the IOLs currently used in clinical

practice are not perfect, and cataract surgery cannot enhance the patient's ability to adjust the lens focus, particularly after surgery. This is because the ciliary muscle connected to the lens capsule is responsible for the focusing, and considering that the ciliary body is also connected to the lens capsule (54), the *in vitro* regeneration of the ciliary body is also related to the lens capsule and lens. We aim to continue investigating the collective regeneration of the lens, lens capsule, and ciliary body *in vitro*. We believe that this can contribute to a finer focus adjustment after IOL implantation if iPS cells can be used to regenerate weakened ciliary bodies.

In conclusion, we have reported that H-iris cells and iris tissue-derived iPS cells can be used to generate a variety of three-dimensional cell aggregates expressing αA-crystallin, a protein specific to the lens. However, all the cell aggregates formed in this study were opaque, and we were thus unable to regenerate a transparent lens. In the future, we will investigate the degradation of organelles necessary to achieve transparency of the interior of the generated cell aggregates expressing lens-specific proteins by creating transgenic cells that induce the disappearance of organelles, and we will conduct research on the regeneration of transparent lenses. In addition, we aim to utilize this cell aggregate model for various applications, such as studying ciliary body regeneration by co-culture and creating an *in vitro* cataract model that can evaluate the effects of drugs and the effects of radiation exposure.

Acknowledgements

The authors would like to thank Ms. Chieko Nishikawa (Fujita Health University) for help with experiments and Ms. Mari Seto (Kanazawa Medical University) for English editing and technical support.

Funding

This research was funded by MEXT/JSPS KAKENHI (grant nos. 17K11495, 20K09838, and 20K09815).

Availability of data and materials

The datasets used and/or analyzed during the current study are available from the corresponding author on reasonable request.

Authors' contributions

NH and NY designed the study. NH, NY and YK were responsible for the data collection and manuscript writing. NH, NY, YK, NN, SI and KI participated in the experiments. NH, YK, NN and SI were responsible for data acquisition and analysis. NY and NN were responsible for statistical analysis. YK and NN were responsible for literature searches. NH, NY, YK and SI reviewed and revised the manuscript. NY and KI confirm the authenticity of all the raw data. All authors have read and approved the final manuscript.

Ethics approval and consent to participate

This study was approved by the Ethics Review Committee of Fujita Health University (approval no. 05-065, first approval date: 21 December 2005, followed by continued ethical approval; Aichi, Japan). The written informed consent was obtained from all subjects. The experiment was carried out with the approval of the Recombinant DNA Experiment Committee of Fujita Health University (approval no. DP16055, approval date: 17 November 2016; Aichi, Japan).

Patient consent for publication

Not applicable.

Competing interests

The authors declare that they have no competing interests.

References

1. Kamachi Y, Uchikawa M, Tanouchi A, Sekido R and Kondoh H: Pax6 and SOX2 form a co-DNA-binding partner complex that regulates initiation of lens development. Genes Dev 15: 1272-1286, 2001.
2. Chow RL and Lang RA: Early eye development in vertebrates. Annu Rev Cell Dev Biol 17: 255-296, 2001.
3. Iribarren R: Crystalline lens and refractive development. Prog Retin Eye Res 47: 86-106, 2015.
4. Morishita H, Eguchi T, Tsukamoto S, Sakamaki Y, Takahashi S, Saito C, Koyama-Honda I and Mizushima N: Organelle degradation in the lens by PLAAT phospholipases. Nature 592: 634-638, 2021.
5. Kuszak JR, Zoltoski RK and Tiedemann CE: Development of lens sutures. Int J Dev Biol 48: 889-902, 2004.
6. Yamamoto N, Tanikawa A and Horiguchi M: Basic study of retinal stem/progenitor cell separation from mouse iris tissue. Med Mol Morphol 43: 139-144, 2010.
7. Griep AE: Cell cycle regulation in the developing lens. Semin Cell Dev Biol 17: 686-697, 2006.
8. Fujii N, Sakaue H, Sasaki H and Fujii N: A rapid, comprehensive liquid chromatography-mass spectrometry (LC-MS)-based survey of the Asp isomers in crystallins from human cataract lenses. J Biol Chem 287: 39992-40002, 2012.
9. Delaye M and Tardieu A: Short-range order of crystallin proteins accounts for eye lens transparency. Nature 302: 415-417, 1983.
10. Magami K, Hachiya N, Morikawa K, Fujii N and Takata T: Isomerization of Asp is essential for assembly of amyloid-like fibrils of αA-crystallin-derived peptide. PLoS One 16: e0250277, 2021.
11. Sprague-Piercy MA, Rocha MA, Kwok AO and Martin RW: α-Crystallins in the vertebrate eye lens: Complex oligomers and molecular chaperones. Annu Rev Phys Chem 72: 143-163, 2021.
12. Takata T, Murakami K, Toyama A and Fujii N: Identification of isomeric aspartate residues in βB2-crystallin from aged human lens. Biochim Biophys Acta Proteins Proteom 1866: 767-774, 2018.
13. Eguchi G, Eguchi Y, Nakamura K, Yadav MC, Millán JL and Tsonis PA: Regenerative capacity in newts is not altered by repeated regeneration and ageing. Nat Commun 2: 384, 2011.
14. Barbosa-Sabanero K, Hoffmann A, Judge C, Lightcap N, Tsonis PA and Del Rio-Tsonis K: Lens and retina regeneration: New perspectives from model organisms. Biochem J 447: 321-334, 2012.
15. Gwon A: Lens regeneration in mammals: A review. Surv Ophthalmol 51: 51-62, 2006.
16. Gwon A, Gruber LJ and Mantras C: Restoring lens capsule integrity enhances lens regeneration in New Zealand albino rabbits and cats. J Cataract Refract Surg 19: 735-746, 1993.
17. Gwon A, Gruber L, Mantras C and Cunanan C: Lens regeneration in New Zealand albino rabbits after endocapsular cataract extraction. Invest Ophthalmol Vis Sci 34: 2124-2129, 1993.
18. Lin H, Ouyang H, Zhu J, Huang S, Liu Z, Chen S, Cao G, Li G, Signer RA, Xu Y, *et al*: Lens regeneration using endogenous stem cells with gain of visual function. Nature 531: 323-328, 2016.
19. Liu X, Zhang M, Liu Y, Challa P, Gonzalez P and Liu Y: Proteomic analysis of regenerated rabbit lenses reveal crystallin expression characteristic of adult rabbits. Mol Vis 14: 2404-2412, 2008.

20. Takahashi K, Tanabe K, Ohnuki M, Narita M, Ichisaka T, Tomoda K and Yamanaka S: Induction of pluripotent stem cells from adult human fibroblasts by defined factors. Cell 131: 861-872, 2007.
21. Chen P, Chen JZ, Shao CY, Li CY, Zhang YD, Lu WJ, Fu Y, Gu P and Fan X: Treatment with retinoic acid and lens epithelial cell-conditioned medium in vitro directed the differentiation of pluripotent stem cells towards corneal endothelial cell-like cells. Exp Ther Med 9: 351-360, 2015.
22. Qiu X, Yang J, Liu T, Jiang Y, Le Q and Lu Y: Efficient generation of lens progenitor cells from cataract patient-specific induced pluripotent stem cells. PLoS One 7: e32612, 2012.
23. Hayashi R, Ishikawa Y, Katori R, Sasamoto Y, Taniwaki Y, Takayanagi H, Tsujikawa M, Sekiguchi K, Quantock AJ and Nishida K: Coordinated generation of multiple ocular-like cell lineages and fabrication of functional corneal epithelial cell sheets from human iPS cells. Nat Protoc 12: 683-696, 2017.
24. Liu Z, Wang R, Lin H and Liu Y: Lens regeneration in humans: Using regenerative potential for tissue repairing. Ann Transl Med 8: 1544, 2020.
25. Sun G, Asami M, Ohta H, Kosaka J and Kosaka M: Retinal stem/progenitor properties of iris pigment epithelial cells. Dev Biol 289: 243-252, 2006.
26. Yamamoto N, Hiramatsu N, Ohkuma M, Hatsusaka N, Takeda S, Nagai N, Miyachi EI, Kondo M, Imaizumi K, Horiguchi M, *et al*: Novel technique for retinal nerve cell regeneration with electrophysiological functions using human iris-derived iPS cells. Cells 10: 743, 2021.
27. Drozd AM, Walczak MP, Piaskowski S, Stoczynska-Fidelus E, Rieske P and Grzela DP: Generation of human iPSCs from cells of fibroblastic and epithelial origin by means of the oriP/EBNA-1 episomal reprogramming system. Stem Cell Res Ther 6: 122, 2015.
28. Yamamoto N, Takeda S, Hatsusaka N, Hiramatsu N, Nagai N, Deguchi S, Nakazawa Y, Takata T, Kodera S, Hirata A, *et al*: Effect of a lens protein in low-temperature culture of novel immortalized human lens epithelial cells (iHLEC-NY2). Cells 9: 2670, 2020.
29. Yang C, Yang Y, Brennan L, Bouhassira EE, Kantorow M and Cvekl A: Efficient generation of lens progenitor cells and lentoid bodies from human embryonic stem cells in chemically defined conditions. FASEB J 24: 3274-3283, 2010.
30. Hayashi R, Ishikawa Y, Sasamoto Y, Katori R, Nomura N, Ichikawa T, Araki S, Soma T, Kawasaki S, Sekiguchi K, *et al*: Co-ordinated ocular development from human iPS cells and recovery of corneal function. Nature 531: 376-380, 2016.
31. Hiramatsu N, Yamamoto N, Isogai S, Onouchi T, Hirayama M, Maeda S, Ina T, Kondo M and Imaizumi K: An analysis of monocytes and dendritic cells differentiated from human peripheral blood monocyte-derived induced pluripotent stem cells. Med Mol Morphol 53: 63-72, 2020.
32. Krogerus L and Kholova I: Cell block in cytological diagnostics: Review of preparatory techniques. Acta Cytol 62: 237-243, 2018.
33. Isogai S, Yamamoto N, Hiramatsu N, Goto Y, Hayashi M, Kondo M and Imaizumi K: Preparation of induced pluripotent stem cells using human peripheral blood monocytes. Cell Reprogram 20: 347-355, 2018.
34. Henry JJ and Hamilton PW: Diverse evolutionary origins and mechanisms of lens regeneration. Mol Biol Evol 35: 1563-1575, 2018.
35. Papaconstantinou J: L.S. stone: Lens regeneration-contributions to the establishment of an in vivo model of transdifferentiation. J Exp Zool A Comp Exp Biol 301: 787-792, 2004.
36. Hayashi T, Mizuno N, Takada R, Takada S and Kondoh H: Determinative role of Wnt signals in dorsal iris-derived lens regeneration in newt eye. Mech Dev 123: 793-800, 2006.
37. Sousounis K, Qi F, Yadav MC, Millán JL, Toyama F, Chiba C, Eguchi Y, Eguchi G, Tsonis PA: A robust transcriptional program in newts undergoing multiple events of lens regeneration throughout their lifespan. Elife 4: e09594, 2015.
38. Eguchi G, Abe SI and Watanabe K: Differentiation of lens-like structures from newt iris epithelial cells in vitro. Proc Natl Acad Sci USA 71: 5052-5056, 1974.
39. Kodama R and Eguchi G: From lens regeneration in the newt to in-vitro transdifferentiation of vertebrate pigmented epithelial cells. Semin Cell Biol 6: 143-149, 1995.
40. Kosaka M, Kodama R and Eguchi G: In vitro culture system for iris-pigmented epithelial cells for molecular analysis of transdifferentiation. Exp Cell Res 245: 245-251, 1998.
41. Abe T, Takeda Y, Yamada K, Akaishi K, Tomita H, Sato M and Tamai M: Cytokine gene expression after subretinal transplantation. Tohoku J Exp Med 189: 179-189, 1999.
42. Yamamoto N, Majima K and Marunouchi T: A study of the proliferating activity in lens epithelium and the identification of tissue-type stem cells. Med Mol Morphol 41: 83-91, 2008.
43. Furukawa KS, Suenaga H, Toita K, Numata A, Tanaka J, Ushida T, Sakai Y and Tateishi T: Rapid and large-scale formation of chondrocyte aggregates by rotational culture. Cell Transplant 12: 475-479, 2003.
44. Nagai T, Furukawa KS, Sato M, Ushida T and Mochida J: Characteristics of a scaffold-free articular chondrocyte plate grown in rotational culture. Tissue Eng Part A 14: 1183-1193, 2008.
45. Duke PJ, Daane EL and Montufar-Solis D: Studies of chondrogenesis in rotating systems. J Cell Biochem 51: 274-282, 1993.
46. Baker TL and Goodwin TJ: Three-dimensional culture of bovine chondrocytes in rotating-wall vessels. In Vitro Cell Dev Biol Anim 33: 358-365, 1997.
47. Marlovits S, Tichy B, Truppe M, Gruber D and Schlegel W: Collagen expression in tissue engineered cartilage of aged human articular chondrocytes in a rotating bioreactor. Int J Artif Organs 26: 319-330, 2003.
48. Cummings CF and Hudson BG: Lens capsule as a model to study type IV collagen. Connect Tissue Res 55: 8-12, 2014.
49. Matsuura-Hachiya Y, Arai KY, Muraguchi T, Sasaki T and Nishiyama T: Type IV collagen aggregates promote keratinocyte proliferation and formation of epidermal layer in human skin equivalents. Exp Dermatol 27: 443-448, 2018.
50. Kelley PB, Sado Y and Duncan MK: Collagen IV in the developing lens capsule. Matrix Biol 21: 415-423, 2002.
51. Nomi K, Hayashi R, Ishikawa Y, Kobayashi Y, Katayama T, Quantock AJ and Nishida K: Generation of functional conjunctival epithelium, including goblet cells, from human iPSCs. Cell Rep 34: 108715, 2021.
52. Barbiero G, Duranti F, Bonelli G, Amenta JS and Baccino FM: Intracellular ionic variations in the apoptotic death of L cells by inhibitors of cell cycle progression. Exp Cell Res 217: 410-418, 1995.
53. de Gann MP, Belaud-Rotureau MA, Voisin P, Leducq N, Belloc F, Canioni P and Diolez P: Flow cytometric analysis of mitochondrial activity in situ: Application to acetylceramide-induced mitochondrial swelling and apoptosis. Cytometry 33: 333-339, 1998.
54. Kinoshita H, Suzuma K, Kaneko J, Mandai M, Kitaoka T and Takahashi M: Induction of functional 3D ciliary epithelium-like structure from mouse induced pluripotent stem cells. Invest Ophthalmol Vis Sci 57: 153-161, 2016.